Life-like Droplets

DOI: 10.1002/anie.201104261

Complex Shapes and Dynamics of Dissolving Drops of Dichloromethane**

Véronique Pimienta, Michèle Brost, Nina Kovalchuk, Stefan Bresch, and Oliver Steinbock**

There is a growing interest in synthetic, chemical systems capable of undergoing autonomous shape changes and/or self-motion.[1] Important examples include solid objects such as catalytic Au/Pt nanorods,[2] mechanically responsive gels driven by oscillating reactions,[3,4] and liquid systems in which self-motion is induced by surface-tension gradients.[5–7] The latter class of systems includes iodine/iodide-containing oil droplets on glass surfaces under aqueous solutions of stearyltrimethylammonium chloride[8] as well as drop motion on an alkylsilane-treated silicon surface with spatial "wettability" changes.[9]

Droplet motion on air–water interfaces is usually driven by a Marangoni effect involving temperature or concentration gradients.[10] A typical example are pentanol droplets on water, which depending on the drop volume, perform erratic or unidirectional motion and also show very disorganized forms of droplet fission.[11] This fission can extend from the millimeter-scale down to nanoscopic micelles.[12]

Herein, we investigate the dynamics of water-saturated dichloromethane (CH_2Cl_2, 25 μL) droplets on aqueous solutions of cetyltrimethylammonium bromide (CTAB). Figure 1 is a qualitative phase diagram describing the macroscopic dynamics in the CH_2Cl_2/CTAB system in terms of the elapsed reaction time and the surfactant concentration. The data are representative for the fourth and fifth drops added. The diagram shows a variety of complex drop shapes and dynamics that we identified to be the most characteristic ones. For each concentration we have studied the dynamics of five successive drops. In general these dichloromethane-accumulating experiments reveal no marked differences; however, the fourth and fifth drops deviate from their predecessors during the late stages of dissolution. These altered dynamics typically match the behavior of drops at a slightly higher CTAB concentration.

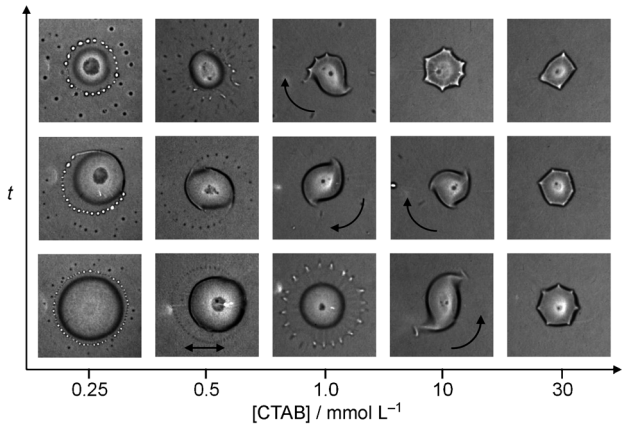

Figure 1. Qualitative description of the drop evolution in the CH_2Cl_2/CTAB system at five different concentrations of the surfactant CTAB. The typical life time of the dissolving droplets ranges between 20 and 90 s. The time axis is not to scale as the diagram emphasizes distinct, successive states in the drop evolution. Single arrows indicate rotation of the drop around its geometrical center. The double arrow indicates that the drop moves back and forth along a fixed line. The field of view of all frames corresponds to 13×13 mm^2.

The life time of the dichloromethane drops varies systematically between approximately 20 and 90 s. This large range is mainly caused by changes in the initial induction period during which drops are stationary and have a circular rim. Complex phenomena are found only for surfactant concentrations above a critical value $[CTAB]_{crit} \approx 0.25$ mmol L^{-1}. In the absence of surfactant or below $[CTAB]_{crit}$, the drops spread out over a large area and solubilize rapidly (< 15 s) without noteworthy macroscopic features. For surfactant concentration close to $[CTAB]_{crit}$ (left column in Figure 1), the initial dichloromethane drops are relatively flat. We also observe that the water surface around the drop supports a disk-shaped film. The macroscopic dynamics involve several successive stages: During the first stage, the edge of the film breaks into small droplets that are continuously ejected and quickly disappear. Then the drop abruptly moves away from the center of the film to maneuver back and forth along a nearly stationary line. During these lateral oscillations, each directional change causes the expulsion of a line of small droplets. After a while, the drop starts to move steadily along a circular orbit larger than its own diameter. Finally all motion ceases, the drop becomes circular again, shrinks and vanishes.

At a surfactant concentration of 0.5 mmol L^{-1} (second column in Figure 1), the dichloromethane drops undergo a similar sequence of motion patterns. However, the dynamics

[*] Prof. Dr. V. Pimienta, Dr. M. Brost
UPS, IMRCP, Université de Toulouse
118 route de Narbonne, 31062 Toulouse Cedex 9 (France)
E-mail: pimienta@chimie.ups-tlse.fr
S. Bresch, Prof. Dr. O. Steinbock
Department of Chemistry and Biochemistry
Florida State University, Tallahassee, FL 32306-4390 (USA)
E-mail: steinbck@chem.fsu.edu
Dr. N. Kovalchuk
Institute of Biocolloid Chemistry
42, Vernadsky av., 03142 Kiev (Ukraine)

[**] We thank David Villa (SPI-FR BT) for backlit photography (Figure 2e,f and S1) and Jean-Claude Micheau for fruitful discussions. We also thank CNES and UFR PCA of Université Paul Sabatier for financial support. O.S. is supported by the National Science Foundation (Grant Nos. CHE-0910657 and DMR-1005861).

Supporting information for this article is available on the WWW under http://dx.doi.org/10.1002/anie.201104261.

commence with the aforementioned lateral oscillations and then give way to drop rotation. The rotating drops eject droplets that form patterns reminiscent of Fibbonacci spirals. For 1 mmol L^{-1} (third column), the initial drop pulsates periodically and its edge is well described by concentric circles of oscillating radius. During this beating motion, the surrounding film spreads periodically and rather violently over larger distances (see also Figure 2 a–d). Close to its maximal extension, the edge of the film breaks into a halo of typically 20–30 droplets and, while recoiling, produces patterns reminiscent of dewetting structures. The period of these phase-locked processes is 0.6–1 s. The drop then transforms into an elongated structure with two sharp tips. This structure rotates in an arbitrary but usually constant direction. Later additional tips form and create asymmetric drop shapes that often transform into rotating drops with three or sometimes four tips. We observe similar structures also at [CTAB] = 10 mmol L^{-1} (fourth column). However, pulsating drops are absent and rotation dominates this intermediate concentration range.

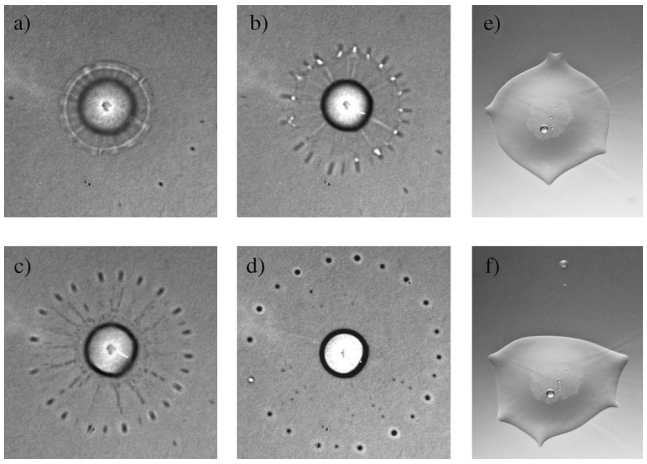

Figure 2. a–d) Image sequence of an early, pulsating drop pattern observed at [CTAB] = 1 mmol L^{-1}. Fast, periodical spreading ejects concentric rings of small droplets. These halos have intricate, internal structures (best seen in frame c). e, f) Emission of a single droplet from a non-rotating polygonal drop at [CTAB] = 30 mmol L^{-1}. The tip-shaped deformations move along the drop's boundary, collide (e), and eject one droplet in an upward direction (f). The photos in (e) and (f) are transmission micrographs of the backlit sample. Field of view and time between frames: 20 × 20 mm^2, 67 ms (a–d) and 15 × 19 mm^2, 111 ms (e, f).

For the highest concentration in Figure 1, dichloromethane drops show neither pulsation nor rotation but have a polygonal rim featuring several small tips. These tips move erratically along the drop boundary and mediate changes in its shape (Figure 2 e). A single small droplet is ejected in radial direction when two tips collide (Figure 2 f). By this mechanism, polygonal drops undergo successive transformations into simpler geometrical structures such as hexagons, pentagons, and finally squares.

In our experiments the rotating two-armed drop is the most frequently encountered and longest lasting structure.

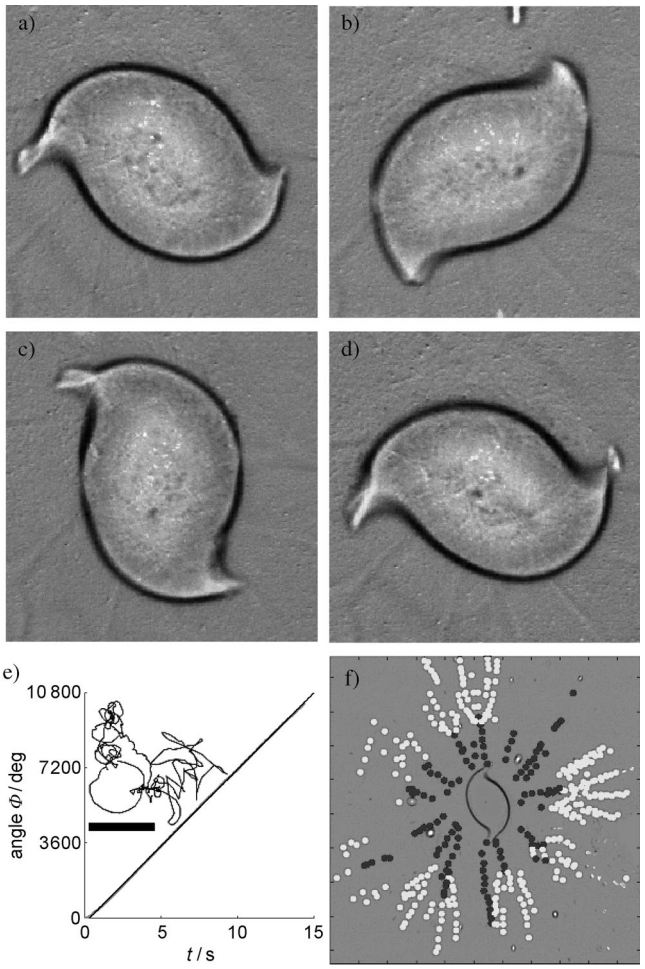

Figure 3. a–d) Image sequence of a rotating, two-armed dichloromethane drop at [CTAB] = 6.8 mmol L^{-1}. Time between frames is 210 ms. Field of view: 9 × 9 mm^2. e) Rotational angle of a similar drop as a function of time and its linear least-square fit (gray line). The inset shows a 21 s-long trajectory of the drop's geometrical center. Scaling bar: 1 mm. f) Snapshot of a rotating two-armed drop at [CTAB] = 6.8 mmol L^{-1}. Superposed are the trajectories of daughter droplets (dark dots) ejected directly by the mother drop and third generation droplets (bright dots) created during the fission of second-generation droplets. Analyzed time interval: 770 ms. Field of view: 17 × 17 mm^2.

Figure 3 a–d shows that the drop shape remains essentially constant under this motion. We characterized its translational movement by computing the geometrical center of the "mother" drop and measured the rotation around this center using a cross-correlation method (see Supporting Information). The resulting data (Figure 3 e) reveal that the drop performs 30 rotations during the course of 15 s at a steady rotation frequency of 1.9 Hz. Simultaneously, its center describes a seemingly erratic trajectory (inset of Figure 3 e) that covers an area much smaller than the drop's footprint. During this remarkably stable rotation, the drop ejects small droplets from its tips with frequencies of up to 30 Hz. The trajectories of these droplets are shown in Figure 3 f (dark dots). Each daughter droplet moves approximately 4 mm, flattens slightly, and then decays into several, even smaller

droplets (bright dots in Figure 3 f), which sometimes split into a fourth (detectable) generation. Notice that the second-generation droplets are ejected in radial direction. Therefore droplet ejection neither drives nor contributes to the generation of rotational motion.

The combination of evaporation, solubilization, and surfactant transfer in the CH_2Cl_2/CTAB system[14] make it highly susceptible to surface-tension-driven thermal[15] and solutal[16] Marangoni instabilities.[17] In this context, the transitions between the distinct drop shapes are closely related to the formation of the surrounding film and its horizontal area. The film is controlled by the spreading power of CH_2Cl_2, which decreases with increasing concentrations of both CTAB and CH_2Cl_2.[18,19] Accordingly, thermal effects are favored at low surfactant concentrations and hence are the likely cause of the lateral and concentric drop oscillations as well as of the associated droplet patterns. For qualitatively similar wetting conditions, Marangoni-driven spreading is also known to induce self-propulsion of aniline drops.[20] Their motion is initiated by an, induced or fortuitous, asymmetry of the spreading film. The resulting imbalance in surface tension is further amplified and sustained by the dissolution of the film in the wake of the moving drop. The same mechanism might explain the laterally oscillating and circling motion patterns in our experiments. However, it clearly fails to account for the observed changes in the film size and the formation of the small droplet patterns.

At higher CTAB concentrations the spreading power of CH_2Cl_2 is low and the drops are more compact. Under such conditions, the solutal Marangoni instability is expected to dominate the system and hence should be a major factor in the observed drop rotation. This interpretation is further supported by our observation of a pair of convection cells within the drop at intermediate CTAB concentrations (see Figure S1 in the supporting information). These cells occupy roughly equal halves of the drop, organize fluid motion at the air/water interface, and are not seen at low concentration. Their faint optical contrast is due to spontaneous emulsification which is rather typical at water-oil interfaces subjected to surfactant transfer.[18]

In summary, we have shown that dichloromethane drops floating on an aqueous CTAB solution can evolve into a surprising range of shapes and motion patterns. The underlying mode selection is very sensitive to the experimental conditions including the concentration of CH_2Cl_2 in the aqueous and gas phase. Despite this limitation, we have identified distinct and novel dynamic states such as symmetrical pulsating drops, multi-armed rotors, and polygonal drops. These shapes are sufficiently stable to undergo dozens of rotation and pulsation cycles or, in the case of the polygonal drops, entertain intricate dynamics of their tips. Coupled to these shape-forming processes is the emission of very small but macroscopic droplets. The droplets can describe linear trajectories and split in a cascading fashion. While linear drop motion had been reported in other systems involving the Marangoni effect, this well-organized cascading decay is an additional novelty. These surprising findings in a seemingly simple system must be related to the specific choice of chemical species. In contrast to many other poorly water-soluble organic solvents, CH_2Cl_2 has a very low boiling point and a high density. Furthermore, we observed similar phenomena in experiments employing the surfactant C_{18}TAB but not for (the nonionic) Brij35.

Experimental Section

All chemicals used are of analytical grade. Cetyltrimethylammonium bromide (CTAB; Aldrich, $\geq 99\,\%$) and dichloromethane (Aldrich, HPLC grade) were used as purchased. The water is ultra-pure (resistivity $> 17\,M\Omega\,cm$). All experiments are carried out at room temperature. The CTAB solution (25 mL) is filled into a cylindrical container (diameter 70 mm) and a single 25 μL drop of CH_2Cl_2 is carefully placed onto the solution surface using a pipette. The system is then covered by a glass plate to reduce matter exchange between the gas layer above the fluid and the surroundings. It is illuminated with white light and the shadow of the floating, lens-shaped drop is monitored from the top with a video camera. Note that the densities of CH_2Cl_2 ($1.33\,g\,mL^{-1}$) and water-saturated CH_2Cl_2 are larger than the density of water.[13] The solubility of dichloromethane in water is $13\,g\,L^{-1}$, which corresponds to a volume 250 μL in 25 mL.

The reproducibility of the experiment is greatly increased by saturating the organic liquid dichloromethane with water. This procedure is used for all experiments and data presented in this study. The solubility of water in CH_2Cl_2 is $2\,g\,L^{-1}$ at 25 °C. The solubility of CH_2Cl_2 in water is $13\,g\,L^{-1}$ ($153\,mmol\,L^{-1}$), which corresponds to a total volume of 0.25 mL in 25 mL of water and, hence, the equivalent of ten of our dichloromethane drops. The solubility of CTAB in water is $15\,g\,L^{-1}$ ($41\,mmol\,L^{-1}$). The partitioning of CTAB between the aqueous and the CH_2Cl_2 phase highly favors the organic liquid.[14] The critical micellar concentration of CTAB in pure water is $0.8\,mmol\,L^{-1}$ ($\gamma_{W/A} = 30.2\,mN\,m^{-1}$). However, in the presence of CH_2Cl_2, an oil-in-water microemulsion is formed and the critical aggregation concentration is decreased to $0.1\,mmol\,L^{-1}$ ($\gamma_{W/A} = 61.5\,mN\,m^{-1}$; $\gamma_{W/O} = 1\,mN\,m^{-1}$). The microemulsion also affects the solubility and solubilization kinetics of CH_2Cl_2 in water.

A typical set of experiments involved five different concentrations of CTAB. For each concentration, the dynamics of five successive droplets were studied. We reproduced these sets of 25 experimental runs several times and on different days. The general succession of patterns is always maintained. The data in Figure 1 are obtained from the fourth or fifth repeat runs. Results obtained at both lower and higher concentration limits have the highest reproducibility.

Received: June 20, 2011
Published online: September 28, 2011

Keywords: liquids · marangoni effect · nonequilibrium processes · self-motion · surfactants

[1] a) C. D. Bain, *ChemPhysChem* **2001**, *2*, 580–582; b) V. M. Starov, *Adv. Colloid Interface Sci.* **2004**, *111*, 3–27; c) S. Karpitschka, H. Riegler, *Langmuir* **2010**, *26*, 11823–11829.
[2] a) W. F. Paxton, K. C. Kistler, C. C. Olmeda, A. Sen, S. K. St Angelo, Y. Y. Cao, T. E. Mallouk, P. E. Lammert, V. H. Crespi, *J. Am. Chem. Soc.* **2004**, *126*, 13424–13431; b) M. Ibele, T. E. Mallouk, A. Sen, *Angew. Chem.* **2009**, *121*, 3358–3362; *Angew. Chem. Int. Ed.* **2009**, *48*, 3308–3312; c) L. F. Valadares, Y. G. Tao, N. S. Zacharia, V. Kitaev, F. Galembeck, R. Kapral, G. A. Ozin, *Small* **2010**, *6*, 565–572.
[3] R. Yoshida, *Adv. Mater.* **2010**, *22*, 3463–3483.
[4] a) V. V. Yashin, A. C. Balazs, *Science* **2006**, *314*, 798–801; b) P. Dayal, O. Kuksenok, A. C. Balazs, *Soft Matter* **2010**, *6*, 768–773.

[5] K. Yoshikawa, N. Magome, *Bull. Chem. Soc. Jpn.* **1993**, *66*, 3352 – 3357.
[6] a) M. M. Hanczyc, T. Toyota, T. Ikegami, N. Packard, T. Sugawara, *J. Am. Chem. Soc.* **2007**, *129*, 9386 – 9391; b) T. Toyota, N. Maru, M. M. Hanczyc, T. Ikegami, T. Sugawara, *J. Am. Chem. Soc.* **2009**, *131*, 5012 – 5013; c) M. Hashimoto, P. Garstecki, H. A. Stone, G. M. Whitesides, *Soft Matter* **2008**, *4*, 1403 – 1413.
[7] H. P. Greenspan, *J. Fluid Mech.* **1978**, *84*, 125 – 143.
[8] Y. Sumino, N. Magome, T. Hamada, K. Yoshikawa, *Phys. Rev. Lett.* **2005**, *94*, 068301.
[9] M. K. Chaudhury, G. M. Whitesides, *Science* **1992**, *256*, 1539 – 1541.
[10] F. Brochard, *Langmuir* **1989**, *5*, 432 – 438.
[11] K. Nagai, Y. Sumino, H. Kitahata, K. Yoshikawa, *Phys. Rev. E* **2005**, *71*, 065301.
[12] K. P. Browne, D. A. Walker, K. J. M. Bishop, B. A. Grzybowski, *Angew. Chem.* **2010**, *122*, 6908 – 6911; *Angew. Chem. Int. Ed.* **2010**, *49*, 6756 – 6759.
[13] *CRC Handbook of Chemistry and Physics*, 87th ed., CRC, Boca Raton, **2004 – 2005**.
[14] R. Tadmouri, C. Zedde, C. Routaboul, J. C. Micheau, V. Pimienta, *J. Phys. Chem. B* **2008**, *112*, 12318 – 12325.
[15] a) V.-M. Ha, C.-L. Lai, *Proc. R. Soc. London Ser. A* **2001**, *457*, 885 – 909; b) A. D. Dussaud, S. M. Troian, S. Harris, *Phys. Fluids* **1998**, *10*, 1588 – 1596.
[16] a) E. Nakache, M. Dupeyrat, M. Vignes-Adler, *J. Colloid Interface Sci.* **1983**, *94*, 187 – 200; b) D. Lavabre, V. Pradines, J.-C. Micheau, V. Pimienta, *J. Phys. Chem. B* **2005**, *109*, 7582 – 7586.
[17] M. Santiago-Rosanne, M. Vignes-Adler, M. G. Velarde, *J. Colloid Interface Sci.* **1997**, *191*, 65 – 80.
[18] J. T. Davies, E. K. Rideal, *Interfacial Phenomena*, Academic Press, New York, **1963**.
[19] D. Bonn, J. Eggers, J. Indekeu, J. Meunier, E. Rolley, *Rev. Mod. Phys.* **2009**, *81*, 739 – 805.
[20] Y.-J. Chen, Y. Nagamine, K. Yoshikawa, *Phys. Rev. E* **2009**, *80*, 016303.

